

## A TWO-STAGE DAMAGE DETECTION METHOD FOR LARGE-SCALE STRUCTURES BY KINETIC AND MODAL STRAIN ENERGIES USING HEURISTIC PARTICLE SWARM OPTIMIZATION

P. Torkzadeh<sup>1</sup>, Y. Goodarzi<sup>2</sup> and E. Salajegheh<sup>1,\*†</sup>

<sup>1</sup> *Department of Civil Engineering, Shahid Bahonar University of Kerman, Kerman, Iran*

<sup>2</sup> *Department of Civil Engineering, Kerman Graduate University of Technology, Kerman, Iran*

### ABSTRACT

In this study, an approach for damage detection of large-scale structures is developed by employing kinetic and modal strain energies and also Heuristic Particle Swarm Optimization (HPSO) algorithm. Kinetic strain energy is employed to determine the location of structural damages. After determining the suspected damage locations, the severity of damages is obtained based on variations of modal strain energy between the analytical models and the responses measured in damaged models using time history dynamic analysis data. In this paper, damages are modeled as a reduction of elasticity modulus of structural elements. The detection of structural damages is formulated as an unconstrained optimization problem that is solved by HPSO algorithm. To evaluate the performance of the proposed method, the results are compared with those provided in previous studies. To demonstrate the ability of this method for detection of multiple structural damages, different types of damage scenarios are considered. The results show that the proposed method can detect the exact locations and the severity of damages with a high accuracy in large-scale structures.

Received: 5 March 2013; Accepted: 25 July 2013

**KEY WORDS:** damage detection; kinetic strain energy; modal strain energy; heuristic particle swarm optimization

---

\* Corresponding author: E. Salajegheh, Department of Civil Engineering, Shahid Bahonar University of Kerman, Kerman, Iran

† E-mail address: eysasala@uk.ac.ir

## 1. INTRODUCTION

Structural damages can be generally detected by comparing properties of the damaged structure with its intact condition. These damages can be represented as small perturbations in properties of the original system such as frequencies, mode shapes and damping, stiffness and plasticity matrices. If variations of the static or dynamic responses for all cases of possible damages are predicted by using an analytical model, the variations of responses measured can be compared with them. For all the variations predicted, the one which is well-matched with the values measured can be identified and the corresponding damage case can be also considered as the real damage of structure. However, the static or dynamic responses will change due to damages dependent on both the damage location and the damage severity [1]. Due to lack of damaged structural responses, the stiffness matrix of the intact structure can be used instead of the stiffness matrix of the damaged structure considering small errors [2].

Several approaches have been proposed to identify the locations and the severity of structural damages, such as that provided by Doebling *et al.* [3]; these methods were based on ranking the modes by using modal strain energy. Shi *et al.* [2] presented a method based on variations of modal strain energy of each element before and after damages. Ghaboussi and Chou [4] used genetic algorithm to detect the damages in a truss structure based on measuring the deflection. The results demonstrated that their method is suitable for detecting the location of damages, although the responses measured were not adequate. Perera *et al.* [5] used particle swarm optimization method in damage detection problems based on multi-objective finite element updating procedure to demonstrate the better performance in comparison with genetic algorithm. Ge *et al.* [6] used the dynamic properties such as frequencies and mode shapes to locate the structural damaged regions. Fang *et al.* [7] utilized the frequency response functions (FRF) as input data using back-propagation neural network and a tunable steepest descent algorithm. Their method could detect the damages with a high accuracy. Wang *et al.* [8] proposed a method based on the modal strain energy of structural elements. They employed a technique incorporated with the singular value decomposition for detecting the location and the severity of damages.

The influence of the model incompleteness and errors were studied in structural damage detection method based on modal data by MotaSoares *et al.* [9]. They utilized the static and dynamic structural responses in various degrees of freedom. The results of their work showed that the dynamic responses have a higher accuracy than the other responses. Seyedpoor [10] considered the structural damage detection as an optimization problem using a two-stage algorithm. In this method, suspected damage elements were identified by using modal strain energy index. The extension of actual damages was also obtained via PSO algorithm. Wang *et al.* [11] utilized the static test data and changes of natural frequencies in structural damage detection. In this method, the damage locations were obtained by using variations in static deformations and natural frequencies. Bakhary *et al.* [12] applied a substructure and multi-stage artificial neural network models to detect the location and the severity of damages. Hong and Karbhari [13] presented the concept of element modal damage index using the modal curvatures. In their proposed method, the damage index was obtained based on modal displacement and modal rotation. Yang [14] applied the use of modal residual force to detect the damage locations and obtaining the damage severities.

Naseralavi *et al.* [15] established an improved genetic algorithm using sensitivity matrix and micro search for structural damage detection. In their method, the sensitivity analysis as an operator was added to the genetic algorithm body. Naseralavi *et al.* [16] presented a strategy for damage detection of cyclic structures based on eigenpair sensitivity matrix. In this method, sensitivity matrices of eigenvalues and pseudo-eigenvectors were established. Beygzadeh *et al.* [17] proposed efficient methods for optimal sensor placement (OSP) based on a new geometrical viewpoint for structural damage detection. Nevertheless, most studies for identification of structural damages have been limited to simple analytical models or simple laboratory tests. In previous studies, damage detection in large-scale structures has been studied less; because there are many difficulties in structural damage detection with increasing the variables (elements).

In this study, a two-stage method is developed based on kinetic and modal strain energy variations and also HPSO algorithm to detect the damages in large-scale structures. The structural damage detection is formulated as an unconstrained optimization problem. Stiffness parameters in finite element model are also considered as the structural damage index.

## 2. DAMAGE LOCATION

The kinetic strain energy is employed to identify the location of damages. In finite element model, the kinetic strain energy of the  $j$ th element in each time of the time history dynamic analysis for the intact and the damaged structure is expressed as follows:

$$U_{jt}^I = \frac{1}{2} \{X_{jt}^I\}^T [K_j] \{X_{jt}^I\} \quad (1)$$

$$U_{jt}^D = \frac{1}{2} \{X_{jt}^D\}^T [K_j] \{X_{jt}^D\} \quad (2)$$

where  $U_{jt}^I$  and  $U_{jt}^D$  are the kinetic strain energy of the intact and the damaged structure and  $X_{jt}^I$  and  $X_{jt}^D$  are the vector of nodal displacements of  $j$ th element at time  $t$  for the intact and the damage structures, respectively, and  $K_j$  is the stiffness matrix of  $j$ th element of structure.

In real structures, damages may have a significant effect on the stiffness. Variation in the stiffness of structure produces variations in the strain energy of elements. For a small perturbation in the stiffness of structure, variation of kinetic strain energy of  $j$ th element at time  $t$  ( $\Delta U_{jt}$ ) is expressed by the following equation:

$$\Delta U_{jt} = \frac{1}{2} \{X_{jt}^D\}^T [K_j] \{X_{jt}^D\} - \frac{1}{2} \{X_{jt}^I\}^T [K_j] \{X_{jt}^I\} \quad (3)$$

It is important to utilize the useful parameters to reduce the possible errors. It is better that  $\Delta U_{jt}$  and  $U_{jt}^I$  are normalized to their maximums in  $j$ th element:

$$\alpha_j = \frac{\Delta U_{jt_{max}}}{\max(\Delta U_{jt_{max}})} \quad (4)$$

$$\beta_j = \frac{U_{jt_{max}}^I}{\max(U_{jt_{max}}^I)} \quad (5)$$

where  $\Delta U_{jt_{max}}$  and  $U_{jt_{max}}^I$  are the maximum of  $\Delta U_{jt}$  and  $U_{jt}^I$  at the various times, respectively, and  $\alpha_j$  and  $\beta_j$  are the normalized  $\Delta U_{jt_{max}}$  and  $U_{jt_{max}}^I$  for  $j$ th the structural element. When damages occur in structural elements, the value of  $\alpha_j$  will increase due to increasing  $U_{jt_{max}}$ . The location of damages is detected with comparison of  $\alpha_j$  and  $\beta_j$ . According to Equations (4) and (5), if the structural elements are intact, the index  $\alpha_j$  will be near zero. Otherwise, the index will be greater than zero for the damaged elements. We decrease the number of variables (elements) by this method.

### 3. DAMAGE SEVERITY

#### 3.1. Modal Strain Energy

If it is assumed that the displacements are corresponding to the mode shapes of the damaged structure, the finite element form of total modal strain energy (MSE) of the  $i$ th mode will be calculated as follows:

$$U^I = \sum_{j=1}^n U_{ji}^I = \sum_{j=1}^n \frac{1}{2} \{\Phi_{ji}^I\}^T [K_j^I] \{\Phi_{ji}^I\} \quad (6)$$

$$U^D = \sum_{j=1}^n U_{ji}^D = \sum_{j=1}^n \frac{1}{2} \{\Phi_{ji}^D\}^T [K_j^D] \{\Phi_{ji}^D\} \quad (7)$$

where  $U^I$  and  $U^D$  are total strain energy of the intact and the damaged structures in  $i$ th mode of the intact and the damaged structures, respectively, and  $\Phi_{ji}^I$  and  $\Phi_{ji}^D$  are the vectors corresponding mode shapes of  $j$ th element in  $i$ th mode of the intact and damaged structure, respectively.

3.2. Objective Function

The goal of the damage detection problem is to determine the location and the severity of damages in the suspected elements based on the specifications measured in the intact structure. The structural damages can generally cause variations of  $\Delta K$  in the stiffness matrix and also variation of MSE in each structural element. If damages occur in structural elements, the total strain energy changes ( $\Delta U$ ) is given by:

$$\Delta U = U^I - U^D \tag{8}$$

If we define the damaged stiffness matrix as  $K_j^D = K_j^I - \Delta K_j$ , then corresponding perturbed matrix of  $j$ th element is  $\Delta K_j = X_j K_j^I$ , where  $X_j \in [0,1]$  is the damage parameter of  $j$ th element. The variation in total MSE of structure can be expressed as the summation of changes in the components of MSE by the following Equations:

$$\Delta U = \sum_{j=1}^n \frac{1}{2} \{ \Phi_{ji}^I \}^T [K_j^I] \{ \Phi_{ji}^I \} - \sum_{j=1}^n \frac{1}{2} \{ \Phi_{ji}^D \}^T [K_j^I - X_j K_j^I] \{ \Phi_{ji}^D \} \tag{9}$$

On the other hand, the total strain energy of the damage structure can be written as:

$$U^D = \frac{1}{2} \{ \Phi_i^D \}^T [K^D] \{ \Phi_i^D \} \tag{10}$$

where  $\Phi_i^D$  is the vector mode shapes of the damaged structure. Therefore, the total strain energy changes are rewritten as:

$$U = \sum_{j=1}^n \frac{1}{2} \{ \Phi_{ji}^I \}^T [K_j^I] \{ \Phi_{ji}^I \} - \frac{1}{2} \{ \Phi_i^D \}^T [K^D] \{ \Phi_i^D \} \tag{11}$$

To find the severity of damages, the objective function is formulated in terms of differences between the finite element and experimental models. Therefore, the objective function depends on the modal strain energy changes. By equaling Equations (9) and (11) we have:

$$\sum_{j=1}^n \delta_j \{ \Phi_{ji}^D \}^T [K_j^I] \{ \Phi_{ji}^D \} = \sum_{j=1}^n \left( \{ \Phi_{ji}^D \}^T [K_j^I] \{ \Phi_{ji}^D \} \right) - \{ \Phi_i^D \}^T [K^D] \{ \Phi_i^D \} \tag{12}$$

The mode shapes are generally normalized with respect to the structural mass. By utilizing the orthogonality of modes and considering  $K^D = M (\omega_i^2)^D$ , Eq. (12) can be written as the following matrix form:

$$[S]\{X\} = \{\Delta R\} \quad (13)$$

The elements of matrix  $[S]$  and vector  $\{\Delta R\}$  can be expressed as follows:

$$S_{ji} = \{\Phi_{ji}^D\}^T [K_j^I] \{\Phi_{ji}^D\} \quad (14)$$

$$\Delta R_j = \sum_{j=1}^n \left( \{\Phi_{ji}^D\}^T [K_j^I] \{\Phi_{ji}^D\} \right) - (\omega_i^2)^D \quad (15)$$

where  $S_{ji}$  is the modal strain energy of the  $j$ th element in  $i$ th mode and  $\Delta R$  is the response changes of the intact and the damaged structure.

The quantity of the error is defined as the difference between the response predicted in the finite element model and the response measured in the damaged structure as follows:

$$e(X) = \Delta R - \hat{\Delta R} \quad (16)$$

where  $\Delta R$  is calculated by using Eq. (15) and  $\hat{\Delta R}$  is the response changes for all suspected damage elements which is obtained from optimization algorithm by solving Eq. (13).

The objective function is defined as follows by an unconstrained optimization problem:

$$\begin{cases} \text{Find: } X_i = \{X_1, X_2, X_3, \dots, X_n\} \\ \text{Minimize: } F(X) = \|SX - \Delta R\|^2 \\ \text{Where: } X_{\min} \leq X \leq X_{\max} \end{cases} \quad (17)$$

where  $F(X)$  is an objective function that should be minimized and  $X_{\min}=1$  and  $X_{\max}=1$  are respectively the lower and upper bounds of the damage vector. In this study, a heuristic particle swarm optimization (HPSO) is employed to determine the damage severity. The damage index  $X_i$  is a parameter which is estimated during the optimization procedure.

By using an optimization algorithm and solving Eq. (13), the damage variables are determined. To achieve the global minimum, the algorithm is performed in several stages and some variables will be eliminated in each stage. In the multi-stage algorithm, first, a number of variables in each stage of HPSO algorithm are considered as suspected damage elements which already have been detected based on section 2. Then, all the intact elements are eliminated in each stage and the algorithm converges to the exact locations and severity of damages. Zero values for the variables represents that the  $i$ th element of structure is intact and a non-zero value refers to the damaged element. If the algorithm does not converge in each stage of optimization, the variables with zero values will be eliminated and will be substituted by the non-zero values as new variables.

### 3.3. Heuristic Particle Swarm Optimization

The heuristic particle swarm optimization (HPSO) is based on the particle swarm optimizer with passive congregation (PSOPC) and harmony search (HS) scheme. The HPSO algorithm handles the problem with specific constraints, using a fly-back mechanism method and the harmony search scheme deals with the variable constraints. The HPSO is initialized with a swarm of random particle and then by using an iteration procedure, the optimum is obtained. In the each iteration, the particles evaluate their fitness (position relative to the goal) and share memories of their best position with the swarm. Subsequently, each particle updates its velocity and position according to the its best previous position, known as *pbest*, and that of the best particle, known as *gbest*, found so far in the swarm. In *k*th iteration, updating of the velocity  $V^i$  and position  $X^i$  of *i*th particle obtained as follows [18]:

$$V_{k+1}^i = WV_k^i + C_1 r_1 (pbest - X_k^i) + C_2 r_2 (gbest - X_k^i) + C_3 r_3 (R_i^k - X_k^i) \quad (18)$$

$$X_{k+1}^i = X_k^i + V_{k+1}^i \quad (19)$$

where  $W$  is an inertia coefficient balancing global and local search,  $r_1$  and  $r_2$  and  $r_3$  are random sequences in the range  $[0, 1]$ ,  $C_1$  and  $C_2$  are the learning and social scaling factors which control the influence of *pbest* and *gbest* on the search process, respectively.  $C_3$  is the passive congregation coefficient and  $R_i$  is a particle selected randomly from the swarm.  $X_i$  and  $V_i$  represent the current position and the velocity of the *i*th particle, respectively.

## 4. MAIN STEPS FOR DAMAGE DETECTION METHOD

The main steps for the proposed damage detection method using HPSO algorithm are summarized as follows:

- (a) Calculating the  $\alpha_j$  and  $\beta_j$  by Equations (4) and (5). In this step, The possible number of damaged elements can be determined by comparing the  $\alpha_j$  and  $\beta_j$ .
- (b) Setting the initial number of design variables equal to the number of suspected damage elements.
- (c) Employing the HPSO to find the optimal solution using a few number of optimization iteration.
- (d) Finding  $i$  as  $x_i=0$  for all components of damage vector and determining the total number of intact elements.
- (e) Removing the intact elements from the damage vector and reducing the variables of optimization problem.
- (f) Performing a new HPSO stage based on the new optimization size to find the optimal solution.
- (g) Checking the convergence by comparing  $\Delta R$  and  $\Delta \hat{R}$ . If two response vectors are identical, saving the results and stopping the optimization process, otherwise, going to the step (d).

## 5. NUMERICAL RESULTS

In this study, three structures are selected as the numerical examples to reveal the robustness and accuracy of the proposed damage detection method. These structures are:

- (1) 31-Bar planer truss
- (2) Double-layer barrel vault with 576 elements
- (3) Double-layer grid with 800 elements

Example 1 is taken from [19] for comparing the efficiency and accuracy of the proposed method with the other existing methods. The second and third examples are chosen arbitrarily. To evaluate the proposed method, time history analysis has been performed. Northridge and Tabas ground motions have been selected from the strong ground motion database of the Pacific Earthquake Engineering Research (PEER) Center [20]. In this study, *MATLAB* [21] is utilized for programming the process while *OpenSees* software [22] is employed for time history dynamic analysis. The mass matrix is also assumed to be constant and the structural damages are simulated as a reduction in the Young's modulus of elements in all examples. The HPSO algorithm parameters for examples have been listed in Table 1.

Table 1: Specifications of the HPSO algorithm

Parameter	Description	Value
NPOP	Number of initial population	50
MNI	Maximum number of iterations	850
C1	Learning parameter	2
C2	Social parameter	2
C3	Passive congregation coefficient	0.01
Wmin	Minimum of inertia weight	0.4
Wmax	Maximum of inertia weigh	0.9

### 5.1. Example 1: 31-bar planer truss

The 31-bar planer truss shown in Figure 1 is selected from [19]. The finite element model has 14 nodes and 28 degrees of freedom. The first ten natural frequencies were utilized for structural damage detection in [19]. The material properties are taken the mass density  $\rho = 2770 \text{ kg} / \text{m}^3$  and the Young's modulus  $E = 70 \text{ GPa}$ . The structure is subjected to the vertical component of Tabas seismic acceleration. Two different damage Scenarios as shown in Table 2 are considered.

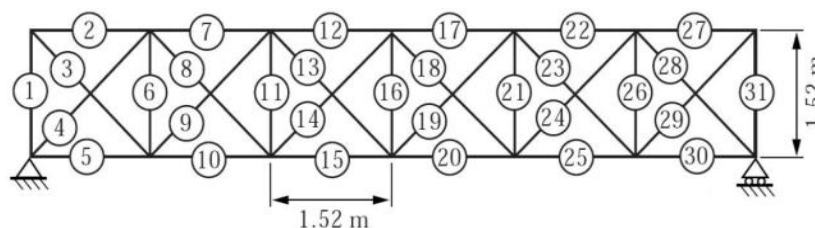


Figure 1. 31-Bar planer truss



Table 2: Two different damages in 31-Bar planer truss

Scenario	Damaged element	Damaged Severity
A	11	25%
	25	15%
B	1	30%
	2	20%

5.1.1. Damage Locations

In this stage of structural damage detection, kinetic strain energies (KSE) of all structural elements are determined for both the intact and the damage structures. Then,  $\alpha_j$  and  $\beta_j$  are evaluated for each structural element through Equations (4) and (5). Then, suspected damage elements are obtained by comparing  $\alpha_j$  and  $\beta_j$  for each element. Figures 2 and 3 show the value of KSE for suspected elements. It can be observed that for the damages considered, the KSE of elements No. 11, 25 in scenario A and elements No. 1, 2, 11 in scenario B of damaged structure are higher than the intact structure.

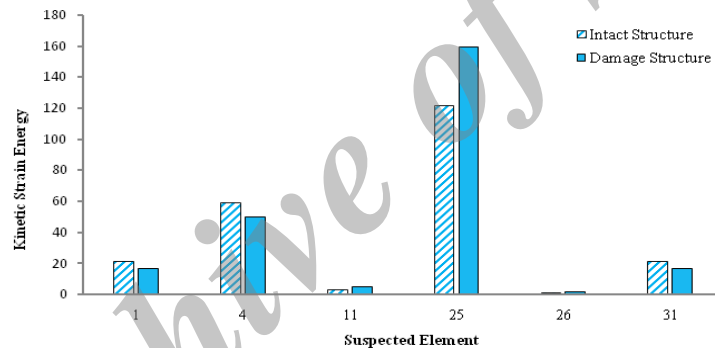


Figure 2. Suspected damage elements in scenario A

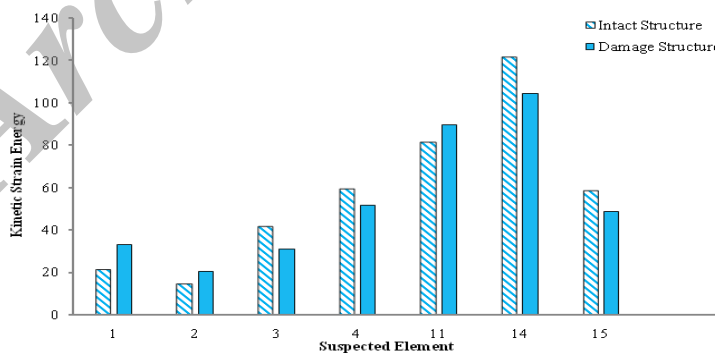


Figure 3. Suspected damage elements in scenario B

5.1.2. Damage Severity by HPSO

After identifying the suspected damages, the damage detection problem reduces to 6 and 7 damaged elements for scenarios A and B, respectively, instead of 31 variables. The HPSO is

employed to find the damage variables through minimizing  $F(x)$  by Eq. (17). In this study, we obtained the damage severity for both scenarios with five mode shapes; while in the method presented in [19] the first ten mode shapes have been employed in calculations. The estimation results of the damage severity are shown in Figures 4 and 5. These figures show that the proposed method results in a more accurate prediction of damage severities than Ref. [19]. The numerical results reveal the high performance of the proposed method for exact detecting the location and severity of various damage scenarios.

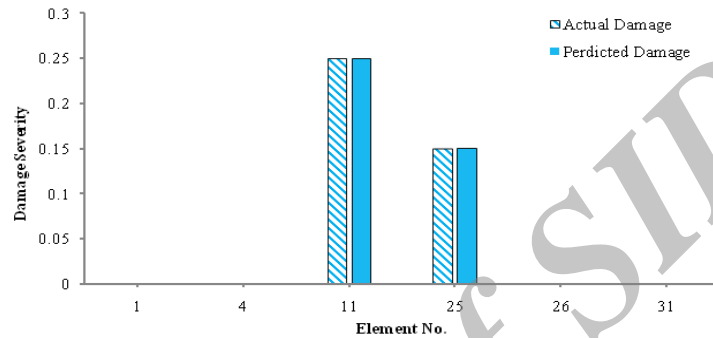


Figure 4. Identified damage elements in scenario A

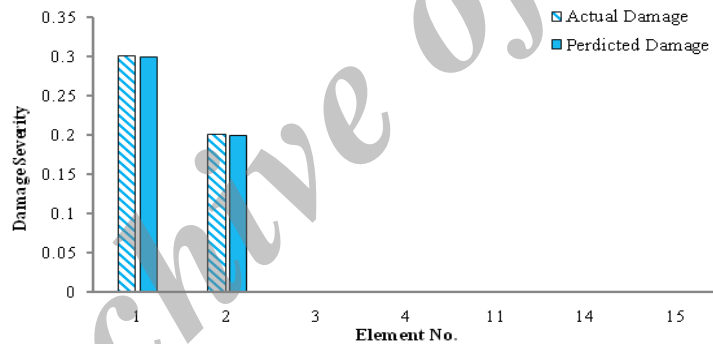


Figure 5. Identified damage elements in scenario B

### 5.2. Example 2: Double-Layer Barrel Vault

In order to represent the high performance of the proposed method for large-scale structures, a double-layer barrel vault with covering surface  $30 \times 40m$  is considered. This space structure with 576 elements and 432 active degrees of freedom is shown in Fig. 6. The cross sectional areas of elements in diagonal, bottom and top layers are  $A_d = 26.75cm^2$ ,  $A_b = 30.43cm^2$  and  $A_t = 39.52cm^2$ , respectively. The mass density and the Young's modulus are assumed to be  $\rho = 7850kg/m^3$  and  $E = 2.1 \times 10^2 GPa$ . Two damage scenarios as shown in Table 3 are assumed in this example. The locations of damaged elements in two scenarios are shown in Figures 7 and 8. The structure is also subjected to the vertical component of Northridge seismic accelerations.

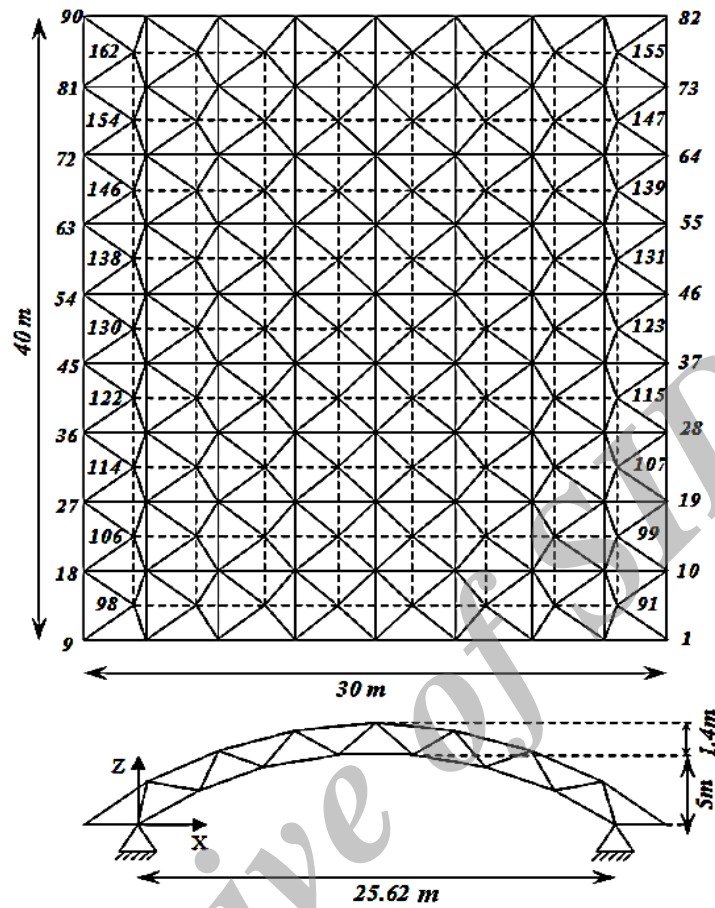


Figure 6. Double-layer barrel vault with 576 elements

Table 3: Damage scenarios in double-layer barrel vault

Scenario	Damaged element	Damaged Severity
A	15	45%
	84	10%
	95	35%
	140	55%
	200	25%
	314	15%
	2	20%
B	10	50%
	48	48%
	66	65%
	84	45%
	120	15%
	164	32%
	282	76%
298	27%	
	556	45%

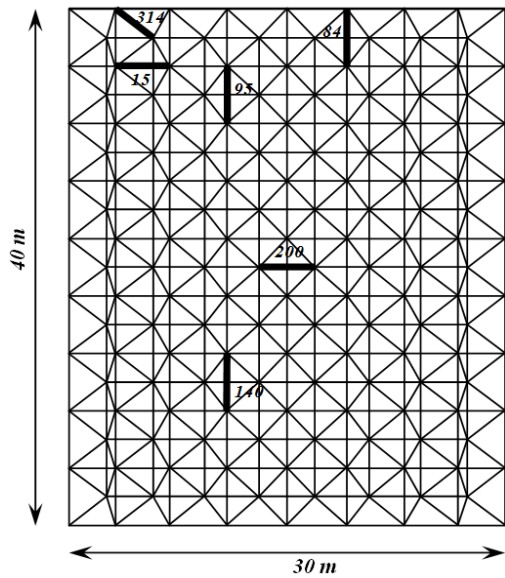


Figure 7. Damaged elements in scenario A

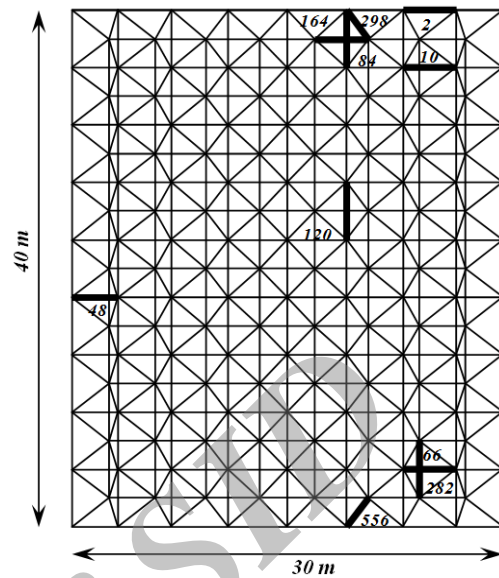


Figure 8. Damaged elements in scenario B

For two damage scenarios,  $\alpha_j$  and  $\beta_j$  for structural elements are determined. The first stage of the proposed method is performed for each scenario and the results are shown in Figures 9 and 10. These figures show that the variables reduce from 576 elements to 19 elements in scenario A and 16 elements in scenario B. Also, these figures represent that the proposed method is very efficient for multiple structural damages; even though the damage severity is low.

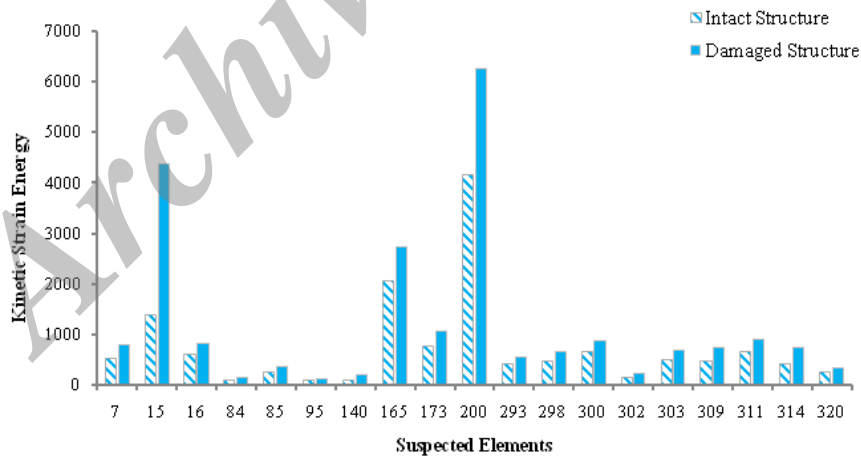


Figure 9. Suspected damage elements in scenario A

In the beginning of the damage severity identification, the number of equations is considered equal to the number of suspected elements. To solve the Equation (13), we employ 19 and 16 mode shapes in scenarios A and B, respectively. The results of damage severities determined in different scenarios are shown in Figures 11 and 12 by using the HPSO algorithm. These figures show that the intact elements are removed in the second

stage of damage detection, though they are chosen as the suspected damage elements in the first stage. Figure 12 represents that the accuracy of the damage severity can slightly decrease when a lot of damaged elements exist; although this is a large-scale structure with a large number of elements.

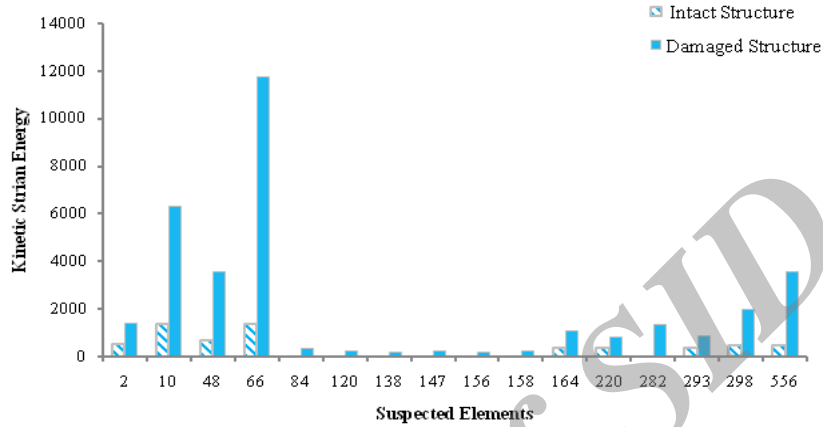


Figure 10. Suspected damage elements in scenario B

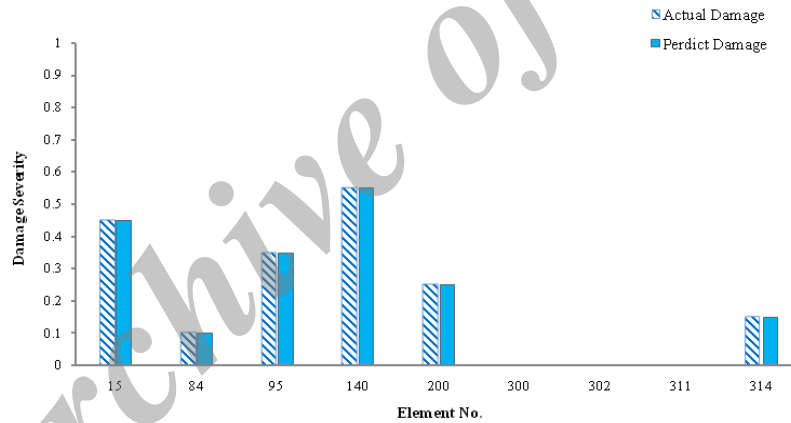


Figure 11. Identified damage elements in scenario A

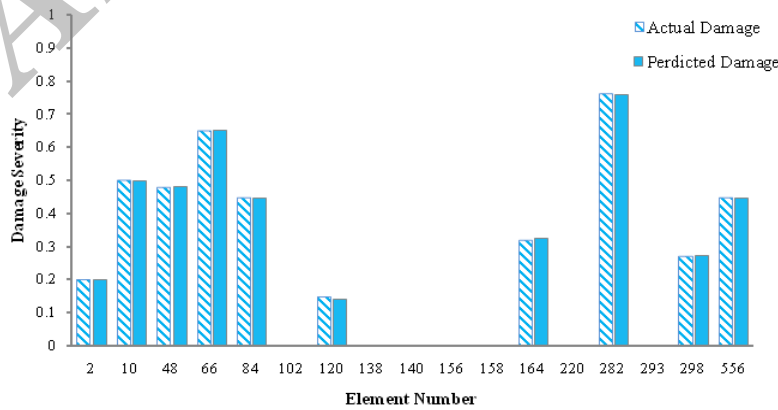


Figure 12. Identified damage elements in scenario B

### 5.3. Example 3: Double-Layer Grid with 800 Elements

To demonstrate the robustness of the proposed method, a double-layer grid with square on square pattern, shown in Figure 13, is considered for damage identification of multiple damage conditions. This space structure has 800 elements and 651 active degrees of freedom. The material properties of elements include Young's modulus of  $E=2.1 \times 10^2 \text{ Gpa}$  and mass density of  $\rho=7850 \text{ kg/m}^3$ . The cross sectional areas of elements in diagonal, bottom and top layers are  $A_d=10 \text{ cm}^2$ ,  $A_b=12 \text{ cm}^2$  and  $A_t=18 \text{ cm}^2$ , respectively. The structure is subjected to the vertical component of Tabas seismic acceleration. Table 4 represents the two types of damage scenarios with different levels of damage severity. The damaged elements are also shown in Figures 14 and 15.

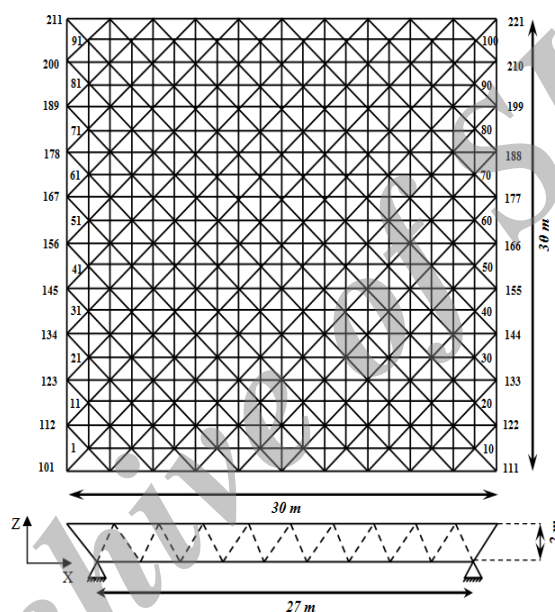


Figure 13. Double-layer grid with 800 elements

Table 4: Damage scenarios in double-layer grid

Scenario	Damaged element	Damaged Severity
A	10	10%
	450	20%
	720	15%
	55	10%
	81	20%
	120	15%
	270	25%
B	300	40%
	400	20%
	500	30%
	600	50%
	700	60%
	800	70%

For scenarios A and B, the modal parameters obtained for the first 10 and 25 modes are used to solve the Equation (13). In the first stage of damage detection, the variables reduce from 800 elements to 32 and 60 elements in scenarios A and B, respectively. The results are obtained for all the 32 and 60 suspected elements by using the frequency changes in the first 10 and 25 modes.

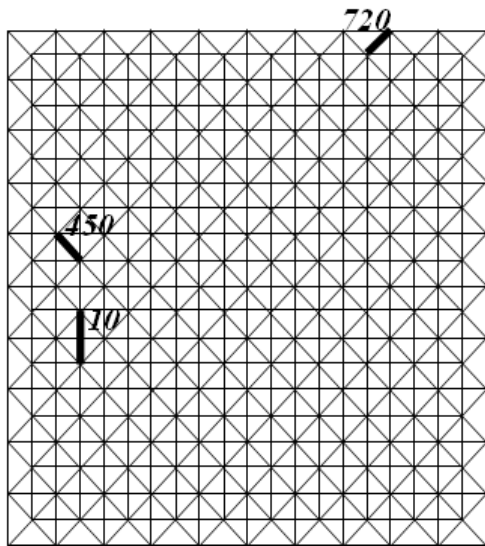


Figure 14. Damaged elements in scenario A

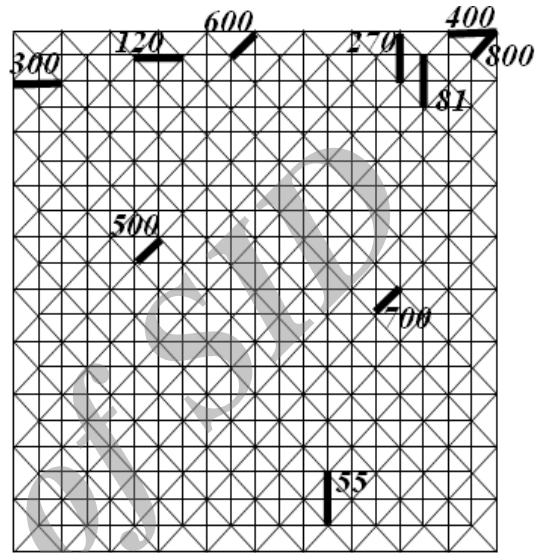


Figure 15. Damaged elements in scenario B

Damage detection results for both damage scenarios are presented in Figures 16 and 17. Figure 17 shows that there is an obvious error in the damage severity of element No. 290. This means that the accuracy of estimated damage severities can slightly decrease when there is a large number of damaged elements. However, this is a large-scale structure with a large number of damaged elements.

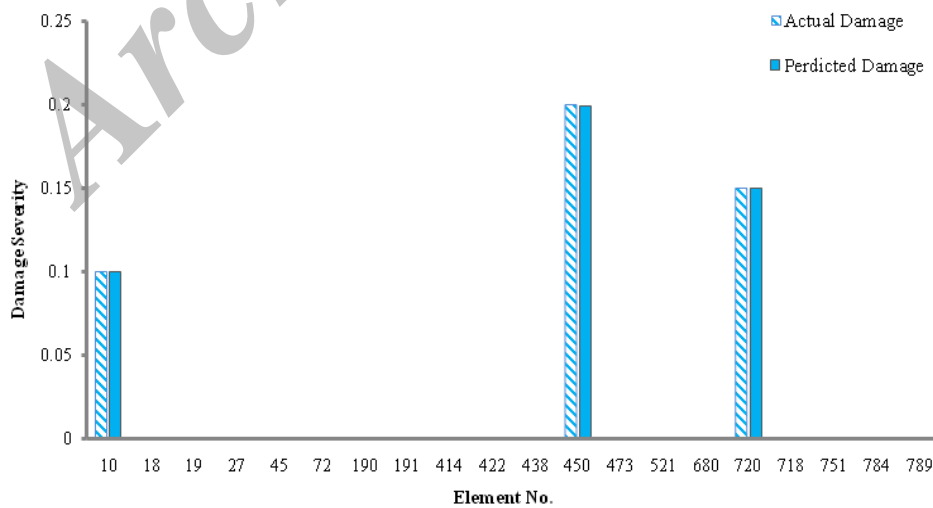


Figure 16. Identified damage elements in scenario A

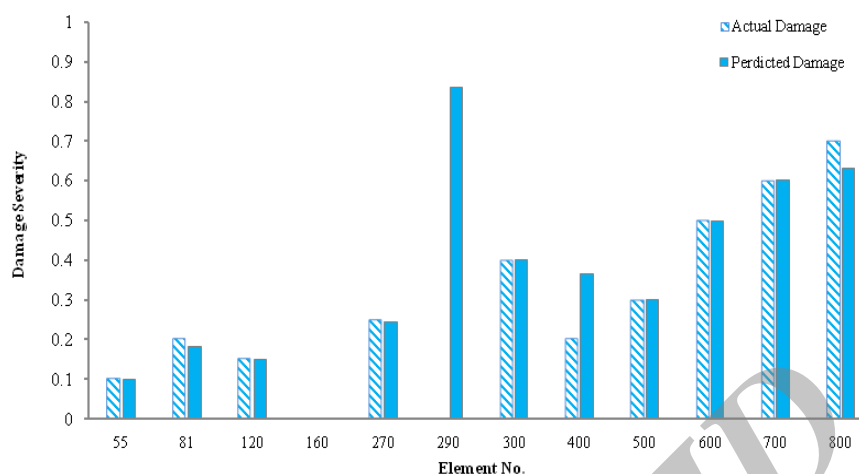


Figure 17. Identified damage elements in scenario B

## 6. CONCLUSION

In this study, a two-stage damage detection method is proposed for large-scale structures. First, the suspected damage locations are detected by comparing the variations in maximum kinetic strain energy of the intact and the damaged structures. Afterwards, the damage severities are obtained by employing the modal strain energy and an iterative optimization algorithm such as HPSO.

The results illustrate the high performance and accuracy of the proposed method for damage detection of large-scale structures with multiple damages. Employing the kinetic strain energy of structural elements in the first stage of damage detection reduces greatly the number of variables from the total elements to a number of suspected damage elements. Moreover, using the MSE values and HPSO algorithm in the second stage of damage detection is more efficient to identify the damage severities; as the suspected damage elements have a higher MSE value than the intact elements.

A large number of structural responses are generally required to identify the damages in large-scale structures such as domes, barrel vaults and double-layer grids. As there is no sufficient available experimental data for structural responses, errors may occur in structural damage detection. The advantage of the proposed method is that the number of required mode shapes to determine the damage severities is considered equal to the number of suspected damage elements. Also, employing HPSO algorithm is effective; because in each step of the process, the dimension of optimization problem is decreased and the numerical instability reaches to the minimum value.

Finally, the results represent that the proposed method can detect the locations and the severity of damages in all damage cases such as small and large damage severities and also multiple damage cases. However, the proposed method is very efficient for damage detection of large-scale structures with a great number of elements and can be used in practical situations.



## REFERENCES

1. Lam HF, Ko JM, Wong CW. Localization of damaged structural connections based on experimental modal and sensitivity analysis, *J Sound Vib*, 1998; **210**: 91-115.
2. Shi ZY, Law SS, Zhang LM. Structural damage detection from modal strain energy changes, *J Eng Mech*, 2000; **126**: 1216-1223.
3. Doebling SW, Peterson LD, Farhat C. Improved damage location accuracy using strain energy based mode selection criteria, *AIAA J*, 1997; **35**: 693-699.
4. Ghaboussi J, Chou JH. Genetic algorithm in structural damage detection, *Comput Struct*, 2001; **79**: 1335-1353.
5. Perera R, Fang SE, Ruiz A. Application of particle swarm optimization and genetic algorithm to multi-objective damage identification inverse problems with modeling errors, *J Springer-Meccanica*, 2010; **45**: 723-734.
6. Ge Ma. Lui EM. Structural damage identification using system dynamic properties, *Comput Struct*, 2005; **83**: 2185-2196.
7. Fang X, Luo H, Tang J. Structural damage detection using neural network with learning rate improvement, *Comput Struct*, 2005; **83**: 2150-2161.
8. Wang JY, Tian LH, Wei, X. Damage detection method based on element modal strain energy sensitivity, *Adv Struct Eng*, 2010; **13**: 1075-1084.
9. MotaSoares CM, Santos JV, MotaSoares CA, Maia, NMM. Structural damage identification: influence of model incompleteness and errors, *Comp Struct*, 2003; **62**: 303-313.
10. Seyedpoor SM. A two stage method for structural damage detection using modal strain energy based index and particle swarm optimization, *Int J Nonlin Mech*, 2012; **47**: 1-8.
11. Wang X, Hu N, Fukunaga H, Yao ZH. Structural damage identification using static test data and changes in frequencies, *Eng Struct*, 2001; **23**: 610-621.
12. Bakhary N, Hao H, Deeks AJ. Structural damage detection using neural network with multi-stage substructuring, *Adv Struct Eng*, 2010; **13**: 1-16.
13. Hong G, Karbhari VM. Improved damage detection method based on element modal strain damage index using sparse measurement, *J Sound Vib*, 2008; **309**: 465-494.
14. Yang QW. A numerical technique for structural damage detection, *Appl Math Comput*, 2009; **215**: 2775-2780.
15. Naserlavi SS, Salajegheh J, Salajegheh E, Fadaee MJ. An improved genetic algorithm using sensitivity analysis and micro search for damage detection, *Asian J Civil Eng*, 2010; **11**: 717-740.
16. Naserlavi SS, Salajegheh E, Salajegheh J, Fadaee MJ. Detection of damage in cyclic structures using an eigenpair sensitivity matrix, *Comput Struct*, 2012; **110**: 43-59.
17. Beygzadeh S, Salajegheh E, Torkzadeh P, Salajegheh J, Naserlavi SS. Optimal sensor placement for damage detection based on a new geometrical viewpoint", *Int J Optim Civil Eng*, 2013; **3**(1): 1-21.
18. Li LJ, Huang ZB, Liu F, Wu QH. A heuristic particle swarm optimizer for optimization of pin connected structures, *Comput Struct*, 2007; **85**: 340-349.
19. Messina A, Williams EJ, Contursi T. Structural damage detection by a sensitivity and statistical-based method, *J Sound Vib*, 1998; **216**: 791-808.
20. [http://peer.berkeley.edu/products/strong\\_ground\\_motion\\_db.html](http://peer.berkeley.edu/products/strong_ground_motion_db.html).

21. The Language of Technical Computing, *MATLAB Math Works Inc*, 2010.
22. Mazzoni S, McKenna F, Fenves GR. OpenSees command language manual-Version 2.2, *University of California- Berkeley*, 2005.

Archive of SID